Materials Research Bulletin 67 (2015) 226–229

Contents lists available at ScienceDirect

Materials Research Bulletin

journal homepage: www.elsevier.com/locate/matresbu

Effect of MgO on microstructure and microwave dielectric properties of $0.84CaTiO_3–0.16Sm_{0.9}Nd_{0.1}AlO_3$ ceramics

Xinye Yang, Xiaohui Wang *, Longtu Li

State Key Laboratory of New Ceramics and Fine Processing, School of Materials Science and Engineering, Tsinghua University, Beijing 100084, China

ARTICLE INFO

Article history:
Available online 30 September 2014

Keywords:
A. Ceramics
C. Electron microscopy
D. Dielectric properties

ABSTRACT

The effect of MgO content on the microstructure and microwave dielectric properties of MgO-doped $0.84CaTiO_3–0.16Sm_{0.9}Nd_{0.1}AlO_3$ ceramics, prepared by solid-state reaction method, was investigated. The permittivity, ε_r, of the MgO-doped $0.84CaTiO_3–0.16Sm_{0.9}Nd_{0.1}AlO_3$ ceramics was about 65, and it decreased slightly with increasing MgO content. And the temperature coefficient of resonant frequency, τ_f was tuned from +53.3 ppm/°C to +26.4 ppm/°C as the MgO addition increasing. In addition, it is found that a small amount of MgO could effectively promote the uniformity of the grain morphology, which is beneficial for the improvement of $Q \times f$ value. However, grain growth was restrained, and secondary phase $MgAl_2O_4$ was observed as MgO content increasing to 0.8 wt%; thus, $Q \times f$ value deteriorated seriously. Considering these three parameters of the microwave dielectric properties, the 0.4 wt% MgO-doped $0.84CaTiO_3–0.16Sm_{0.9}Nd_{0.1}AlO_3$ ceramics exhibited the best performance of $\varepsilon_r = 64.21$, $Q \times f =$ 30867 GHz, and $\tau_f = 26.4$ ppm/°C sintered at 1375 °C for 3 h.

1. Introduction

The rapid progress of the third generation to the fourth generation telecommunication has driven the improvement of microwave dielectric ceramics used for base station in cellular networks. Three key property parameters are paid much attention [1–3]. They include high permittivity, ε_r, to reduce the size of a circuit, high quality factor, $Q \times f$, which is necessary for frequency selectivity, and near-zero temperature coefficient of the resonator frequency, τ_f, to prevent frequency drifting. Most commercial materials have a permittivity around 40, such as $Ba(Co, Zn)_{1/3}Nb_{2/3}O_3$ [4,5], $CaTiO_3–NdAlO_3$ [6–8], and $(Zr, Sn)TiO_4$ [2,9]. In the light of the demand to minimize the size of microwave devices, permittivity should be higher. However, materials with permittivity between 50 and 70 have not been extensively studied. This is because high $Q \times f$ and zero τ_f were hardly obtained simultaneously [10–13].

Solid solution materials are formed between one positive τ_f and another negative τ_f material to tailor the dielectric properties. For example, the properties of $xCaTiO_3–(1-x)LnAlO_3$ (Ln = La, Nd, Sm) solid solution can be tuned between two end compositions [14–18]. Considering that $CaTiO_3$ has $\varepsilon_r = 170$ and $SmAlO_3$ has $\varepsilon_r = 20.4$, the permittivity varies in a wide range from 20 to 70 with the ratio of two end members and it was found that $0.84CaTiO_3–0.16SmAlO_3$ has permittivity around 65 [19–21]. Therefore, it is significant to design materials with permittivity between 50 and 70 in $xCaTiO_3–(1-x)SmAlO_3$ solid solutions.

In this work, MgO doped $0.84CaTiO_3–0.16Sm_{0.9}Nd_{0.1}AlO_3$ solid solution was prepared by conventional solid-state reaction method. The effect of Mg dopant on structure and dielectric properties was investigated.

2. Experimental procedure

To prepare MgO doped $0.84CaTiO_3–0.16Sm_{0.9}Nd_{0.1}AlO_3$ (0.84CTSA) ceramics, $CaTiO_3$ and $Sm_{0.9}Nd_{0.1}AlO_3$ were synthesized respectively. Starting materials included Sm_2O_3, Nd_2O_3, Al_2O_3, $CaCO_3$, TiO_2, and MgO powders with high-purity (99.9%). $CaTiO_3$ and $Sm_{0.9}Nd_{0.1}AlO_3$ were weighed separately according to the stoichiometric composition. The blended powders were then milled with ZrO_2 balls in deionized water for 24 h, dried and calcined at 1170 °C for 3 h.

According to the formula of $0.84CaTiO_3–0.16Sm_{0.9}Nd_{0.1}AlO_3$, $Sm_{0.9}Nd_{0.1}AlO_3$ and $CaTiO_3$ were mixed with various amount of MgO (x wt%, $x = 0–2$) and ball milled again for 12 h. The obtained powders were pressed into 10-mm diameter, 5–6-mm thick pellets at 200 MPa. The pellets were finally sintered at different temperatures from 1355 °C to 1395 °C for 3 h in air.

The crystal structures of samples were investigated using an X-ray diffraction (XRD) instrument (D/max 2500, Rigaku, Japan)

---

* Corresponding author. Tel.: +86 10 62784579; fax: +86 10 62771160.
E-mail address: wxh@mail.tsinghua.edu.cn (X. Wang).

http://dx.doi.org/10.1016/j.materresbull.2014.09.082
0025-5408/

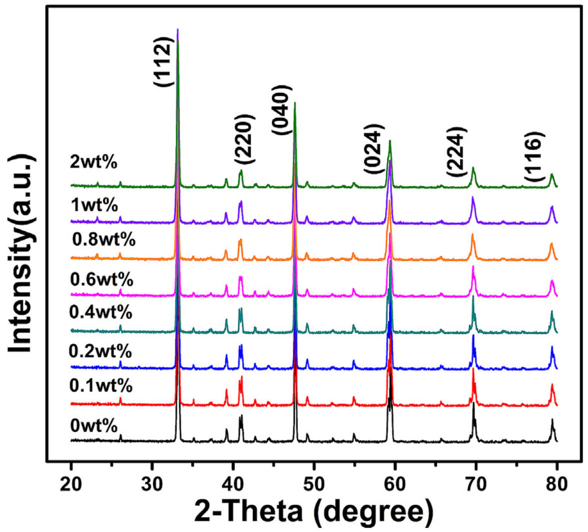

Fig. 1. XRD patterns of $0.84CaTiO_3$–$0.16Sm_{0.9}Nd_{0.1}AlO_3$ ceramics added with x wt% MgO.

with Cu Kα radiation. The microstructures of the ceramic specimens were observed by a scanning electron microscope (SEM, JSM-7001F, JEOL, Japan) and transmission electron microscopy (TEM, Tecnai G20, FEI, USA). The microwave dielectric properties of the ceramic specimens were evaluated using a network analyzer (HP8720ES, Hewlett-Packard, USA). The dielectric constants were measured by the Hakki–Coleman dielectric resonator method with the TE_{011} mode [22,23], and the unloaded quality factors were measured using the $TE_{01\delta}$ mode in the cavity method [24]. The τ_f values of the samples were obtained by the cavity method in the temperature range from 25 to 80 °C.

3. Results and discussion

Fig. 1 shows the XRD patterns of 0.84CTSA ceramics added with various amount of MgO sintered at 1375 °C. It can be seen that a perovskite phase was obtained. No apparent variation was observed.

Fig. 2 shows the SEM images of x wt% MgO-doped 0.84CTSA ceramics sintered at 1375 °C. All the samples are well sintered, and dense microstructure are obtained. The grains become more homogeneous as MgO amount is increased. However, for the specimen with $x = 0.8$ and $x = 2$, the grain size decreases to 2 μm. This result implied that the addition of MgO hinders the migration of grain boundaries in 0.84CTSA ceramics, by which the homogeneity is improved and the grain growth is suppressed. Notably, a secondary phase could be observed along the grain boundaries in specimen with $x = 0.8$ and $x = 2$, which was identified by energy dispersive spectroscopy (EDS).

Fig. 3 shows the element mapping report for the polished and thermally etched surface of 0.84CTSA + 0.8 wt% MgO sample by SEM-EDS. Obviously, the secondary phase along the grain boundaries is rich in Mg and Al and lack of Ca and Ti. Apart from that, the EDS mapping result also shows a uniform distribution of Mg element throughout the parent phase. Comparing the ionic radii of all constituent elements in specimen [25], it is clear that the doped Mg ions have a solubility limit in 0.84CTSA. When the addition is above the limit, the excessive Mg ions might segregate in grain boundaries; thus, secondary phase is formed.

To further confirm the composition and structure of the secondary phase, a more detailed TEM study was performed. Fig. 4(a) shows a TEM image of the secondary phase in 0.84CTSA + 0.8 wt% MgO, and the insert is a SAED (selected area electron diffraction) pattern collected along [0 0 1] zone axis. According to the TEM-EDS analysis shown in Fig. 4(b), the composition of the secondary phase is $MgAl_2O_4$. In addition, the spinel $MgAl_2O_4$ phase (space group $Fd\overline{3}m$, lattice constant $a = 8.0831$ Å) shows good consistence with the electron diffraction pattern. Consequently, it can be confirmed that these secondary phases are true $MgAl_2O_4$ phase. However, the concentration of $MgAl_2O_4$ phase is relatively low, so it is not detected by XRD analysis due to its high detection limit.

Fig. 5 shows the microwave dielectric properties of the specimens sintered at different temperatures as a function of MgO addition x. Permittivity ε_r decreases from 65.5 to 63 with the increase of x value. Generally, permittivity depends on the relative density and ionic polarizability at microwave frequencies [2,26]. The relative density could be ignored due to the dense microstructure observed by SEM. The polarizability, α_i, is correlated with ε_r by Classius–Mosotti equation [27],

$$\frac{\varepsilon_r - 1}{\varepsilon_r + 2} = \frac{4\pi}{3}\sum N_i\alpha_i$$

where N_i is the concentration of atoms. Since the polarizablity of Mg^{2+} (1.32 Å^3) is smaller than Ca^{2+} (3.16 Å) and Ti^{4+} (2.98 Å) [28], the polarizability of specimen decreases as MgO content increases. Accordingly, permittivity ε_r decreases with the polarizability. In addition, ε_r is affected by secondary phases simultaneously. According to the Lichitenecher logarithm rule [29], the appearance of $MgAl_2O_4$ with a low permittivity ($\varepsilon_r = 8.8$) diminishes the permittivity when x is over 0.8. A slight increase in permittivity for the specimen with $x = 0.6$ is caused by Mg^{2+} solubility limit. The variation of the temperature coefficient of the resonant frequency,

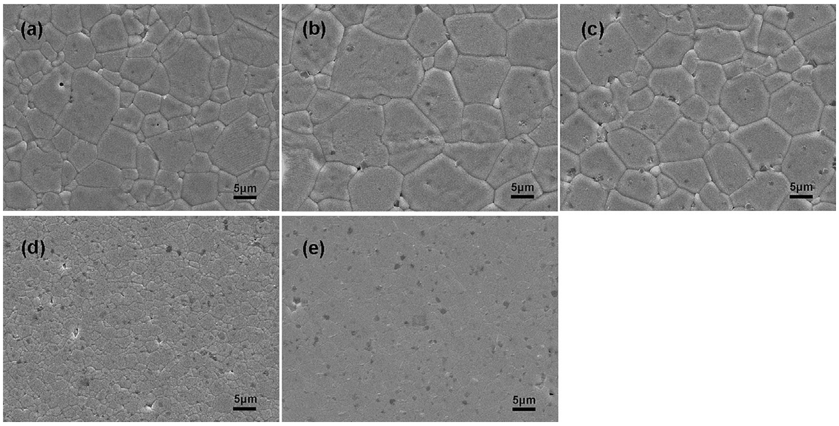

Fig. 2. SEM micrographs of $0.84CaTiO_3$–$0.16Sm_{0.9}Nd_{0.1}AlO_3$ ceramics added with x wt% MgO sintered at 1375 °C: (a) $x = 0$; (b) $x = 0.2$; (c) $x = 0.6$; (d) $x = 0.8$; (e) $x = 2$.